Intermediate mass muon pair continuum in Pb–Pb collisions at 158 GeV/c

Presented by Enrico Scomparin for the NA50 collaboration

M.C. Abreu[6], C. Alexa[2], B. Alessandro[11], J. Astruc[8], C. Baglin[1], A. Baldit[4], F. Bellaiche[12], M. Bedjidian[12], S. Beolè[11], A. Borhani[9], V. Boldea[2], G. Bonazzola[11], P. Bordalo[6], A. Bussière[1], V. Capony[1], J. Castor[4], M. Cerú[3], T. Chambon[4], B. Chaurand[9], I. Chevrot[4], B. Cheynis[12], E. Chiavassa[11], C. Cicalo[3], S. Constantinescu[2], W. Dabrowski[11], A. De Falco[3], G. Dellacasa[11], N. De Marco[11], A. Devaux[4], S. Dita[2], O. Drapier[12], B. Espagnon[4], J. Fargeix[4], F. Fleuret[9], P. Force[4], M. Gallio[11], Y.K. Gavrilov[7], C. Gerschel[8], P. Giubellino[11], M.B. Golubeva[7], M. Gonin[9], P. Gorodetzky[10], J.Y. Grossiord[12], P. Guaita[11], F.F. Guber[7], A. Guichard[12], R. Haroutunian[12], M. Idzik[11], D. Jouan[8], T.L. Karavitcheva[7], R. Kossakowski[1], L. Kluberg[9], A.B. Kurepin[7], Y. Le Bornec[8], G. Landaud[4], C. Lourenço[5], L. Luquin[4], P. Macciotta[3], F. Ohlsson-Malek[12], A. Marzari-Chiesa[11], M. Masera[11], A. Masoni[3] , S. Mourgues[4], A. Musso[11], P. Petiau[9], W.L. Prado da Silva[11a], A. Piccotti[11], J.R. Pizzi[12], G. Puddu[3], C. Racca[10], L. Ramello[11], S. Ramos[6], P. Rato-Mendes[11], L. Riccati[11], A. Romana[9], M.S. Sartori[11], P. Saturnini[4], E. Scomparin[11], R. Shaoian[5], S. Silva[6], S. Serci[3], P. Sonderegger[5], X. Tarrago[8], P.Temnikov[3], N.S. Topilskaya[7], G. Usai[3], E. Vercellin[11], and N. Willis[8].

[1] LAPP, CNRS-IN2P3, F-74019 Annecy-le-Vieux, France.
[2] IFA, R-76900 Bucharest, Romania.
[3] Università di Cagliari/INFN, I-09127 Cagliari, Italy.
[4] LPC, Univ. de Clermont-Ferrand and CNRS-IN2P3, F-63177 France.
[5] CERN, CH-1211 Geneva 23, Switzerland.
[6] LIP, P-1000 Lisbon, Portugal.
[7] INR, 117312 Moscow, Russia.
[8] IPN, Univ. de Paris-Sud and CNRS-IN2P3, F-91406 Orsay, France.
[9] LPNHE, Ecole Polytechnique and CNRS-IN2P3, F-91128 Palaiseau, France.
[10] CRN, CNRS-IN2P3 and Univ. Louis Pasteur, F-67037 Strasbourg, France.
[11] Università di Torino/INFN, I-10125 Torino, Italy
[12] IPN, Univ. de Lyon and CNRS-IN2P3, F-69622 Villeurbanne, France.
[a] Now at UERJ, Rio de Janeiro, Brazil

The NA50 experiment measures, at CERN SPS, the dimuon production in Pb–Pb collisions at 158 GeV/c incident momentum. In this paper an analysis of the intermediate mass region ($1.5 \leq M_{\mu\mu} \leq 2.5$ GeV/c^2) is presented. Known dimuon sources in this interval of the spectrum are the e.m. annihilation of $q\overline{q}$ pairs (i.e. Drell-Yan) and the semi-leptonic decay of charmed hadrons. The contribution of these processes is calculated by means of a fit to the measured invariant mass distribution (for Drell-Yan) and of a linear extrapolation of p–A experimental results obtained by NA38 (for charm). It will be shown that known sources do not account for all of the dimuon yield measured by NA50, i.e. an excess is observed. The size of the excess measured in Pb–Pb is larger than the one seen by NA38 in S–U collisions. The centrality dependence of this effect, both in S–U and Pb–Pb, is also discussed.

1. EXPERIMENTAL SETUP AND DATA-TAKING CONDITIONS

The NA50 experiment is basically an upgrade of NA38, which measured dimuon production using protons and ions (^{16}O, ^{32}S) as projectiles. Due to the increase in the hadron multiplicity in Pb-induced collisions as compared to light ions, some detectors had to be modified; moreover, devices which are situated close to the beam axis have been built using radiation resistant materials.

The main detector is a muon spectrometer[1], which detects dimuons in the rapidity range $2.7 < y_{lab} < 3.9$. The muon tracks are deflected by a toroidal magnetic field, and reconstructed using two sets of four MWPC; two sets of two scintillator hodoscopes provide the trigger signal for the experiment.

The spectrometer is separated from the target region by a 4 m long hadron absorber made of carbon, followed by 80 cm of iron. A uranium central plug absorbs the projectile spectators and the beam particles which do not interact in the target.

A segmented active target (20% interaction length), consisting of seven sub-targets, each one followed by two quartz blades located slightly off the beam axis, provides the identification of the interaction point.

A beam hodoscope (BH), located 33 m upstream from the target, in a region where the beam spot is large enough so that individual incoming ions can be tagged, provides the counting of incident ions and allows pile-up rejection. This detector is made of a plane of 16 quartz blades.

The centrality of the collision is measured using three different detectors, namely:

an electromagnetic calorimeter (EMC), positioned in front of the hadron absorber, out of the spectrometer's acceptance, and made of scintillating fibers embedded in lead, which measures the neutral transverse energy E_T^0 produced in the pseudo-rapidity range $1.1 < \eta_{lab} < 2.3$;

a zero degree calorimeter (ZDC)[2], made of quartz fibers embedded in tantalum, which measures the energy E_{ZDC} not involved in the collision, providing a direct estimate of the number of projectile spectators; this detector is placed on the beam axis inside the hadron absorber, in front of the central uranium plug and receives a monthly dose of about 1.8 Grad;

a multiplicity detector (MD)[3], made of two planes of silicon strip detectors and positioned immediately after the target system, which measures the charged hadron multiplicity in the pseudo-rapidity interval $1.6 < \eta_{lab} < 4.0$.

The whole apparatus is designed in order to stand high incident beam rate ($> 10^7$

ions/burst); this requirement is essential because of the low probability to produce a muon pair in hadronic interactions.

A preliminary run with Pb ions in 1994 was mainly devoted to the setting-up of the various detectors. In 1995, during a 40 days beam period, working at a beam intensity of about $4{\cdot}10^7$ Pb ions per burst (of about 5 s) $4.7{\cdot}10^7$ triggers have been collected on tape, making possible a first physics analysis.

2. DATA REDUCTION

The analysis has been carried out on a sample of $1.7{\cdot}10^7$ dimuon events, corresponding to stable beam conditions and detector performances. Both opposite-sign (OS) and like-sign (LS) dimuons have been recorded, since the latter are used to estimate the fraction of OS events coming from uncorrelated π and K decays.

In order to reject dimuons coming from kinematical regions where the acceptance is very low, only events which satisfy the cuts $0 \leq y^* \leq 1$, $-0.5 \leq cos\theta_{CS} \leq 0.5$, where y^* is the dimuon CM rapidity and θ_{CS} is the decay angle of the μ^+(if there is one) relative to the beam direction in the muon pair rest frame (Collins–Soper reference frame), have been selected for the analysis. No cut on p_T variable has been introduced.

Only events where the incident Pb ion has interacted in one of the seven subtargets have been retained. The interaction in a given target is recognized when both quartz blades looking at that target have detected a signal exceeding a threshold; such a threshold has been chosen in order for the system to identify peripheral Pb–Pb collisions, without being sensitive to δ-rays produced by non-hadronic interactions of the incident ion. The average efficiency of the active target system for Pb–Pb interactions producing a dimuon turns out to be 81±3%.

A set of veto counters identifies 'halo' events where the Pb ion does not cross the targets, which are rejected.

The Beam Hodoscope recognizes events with a second incident Pb ion in a 10 ns time window around trigger time. Since such an ion can bias the information from the various detectors which measure the collision geometry (EMC, ZDC, MD), these pile-up events (about 20%) are rejected from the sample used for the study of the centrality dependence of dimuon production.

Finally, the analysis has been restricted to the region $M_{\mu\mu} \geq 1.5$ GeV/c^2, since for lower mass values the contribution to the dimuon spectrum from decays of vector mesons (ρ, ϕ), is no longer negligible, and dimuon sources different from Drell-Yan and open charm decays would have to be taken into account.

The $\mu^+\mu^-$ mass spectrum, after data reduction, contains $4.5{\cdot}10^5$ events. It is shown in fig. 1 and appears as a wide mass continuum dominated by the J/ψ peak. A shoulder around $M_{\mu\mu}$=3.8 GeV/c^2, corresponding to the decay $\psi' \rightarrow \mu^+\mu^-$, is also clearly visible.

2.1. Background subtraction

In the intermediate mass region a large fraction of the OS events comes from uncorrelated muon pairs produced by in-flight decays of π and K mesons (combinatorial background). Since recorded events include also like-sign dimuons, entirely due to such processes, the standard formula

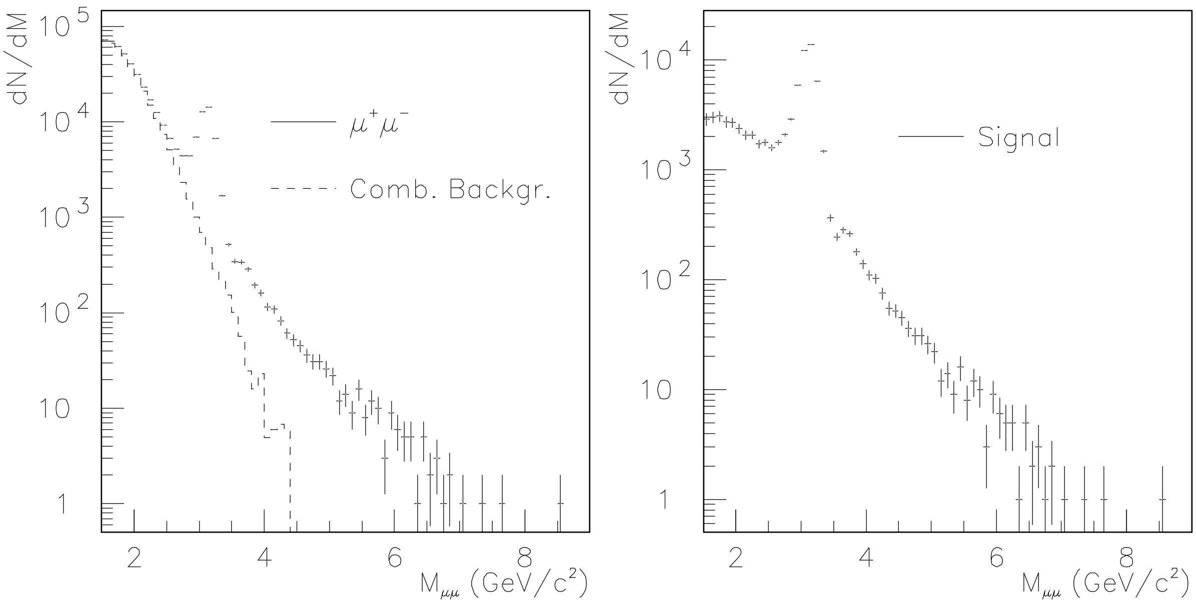

Figure 1. Dimuon mass distribution in Pb–Pb collisions.

$$N^{+-}_{BCK} = 2 \cdot R_{BCK}\sqrt{N^{++}N^{--}}$$

has been used to subtract, bin per bin, the background contribution N^{+-}_{BCK} to the OS spectrum. N^{++} and N^{--} are extracted directly from LS mass distributions. The value of R_{BCK} can differ from unity only if there is an acceptance bias relatively to the muon charge, i.e. the apparatus treats in a different way μ^+ and μ^-, or if the multiplicity of the parent π and K is low.

In order to remove this kind of acceptance bias a further cut is applied (image cut) which discards events which would not be accepted by the spectrometer if the charge of the two muons were exchanged.

Finally, a Monte-Carlo simulation, based on Fritiof event generator, shows that nucleus–nucleus hadron multiplicities (already for nuclear systems much smaller than Pb, such as sulphur) allow to choose $R_{BCK} = 1$.

The estimated background contribution amounts to about 90% of the OS spectrum in the intermediate mass region. The 'signal' spectrum $N^{+-}_{sig} = N^{+-} - N^{+-}_{BCK}$ is shown in fig. 1, and is the starting point for the following analysis.

3. THE ANALYSIS

3.1. Introduction

The aim of this analysis is to describe the signal mass spectrum measured by NA50 and shown in fig. 1 in terms of known dimuon sources; in the considered mass region ($M \geq 1.5$ GeV/c^2) they are assumed to be Drell-Yan (DY), the $J/\psi \to \mu^+\mu^-$ and $\psi' \to \mu^+\mu^-$ decays, and the semi–leptonic decay of couples of charmed hadrons ($D\overline{D}$).

The shape of the dimuon invariant mass distribution generated by each process has been obtained by means of a Monte-Carlo simulation.

The normalizations of the various sources is then obtained:
– for DY, J/ψ, ψ', by a fit to the high mass tail of the experimental spectrum;
– for $D\overline{D}$ by a linear extrapolation of the yield measured by NA38 in p–W collisions at 200 GeV.

Finally, the sum of these expected contributions is compared with the signal mass spectrum of fig. 1.

3.2. Differential spectra

For each of the four processes contributing to the invariant mass spectrum, events were generated according to distributions of the kinematical variables which are empirical parametrizations of differential cross sections or results of QED calculations (for DY). θ_{CS} spectra are obtained from simple angular momentum considerations. The following choices[4] have been made:

a) J/ψ and ψ'

– M: constant (3.097 GeV/c^2 for the J/ψ and 3.686 GeV/c^2 for the ψ').

– y^*: gaussian with μ_{y^*}=0 and σ_{y^*}=0.6 .

– p_T: $p_T m_T K_1(m_T/T)$, where K_1 is the second modified Bessel function of order 1, and T=0.236 GeV.

– $cos\theta_{CS}$: uniform.

b) Drell-Yan

– M, y^*: according to the lowest order QED formula, for colliding nucleons A and B:

$$M^3\frac{d^2\sigma}{dMdy^*} = \frac{8\pi\alpha^2}{9}\tau\Sigma_f(\frac{e_f}{e})^2[q_f^B(\sqrt{\tau}e^{y^*})\cdot\overline{q}_f^A(\sqrt{\tau}e^{-y^*}) + \overline{q}_f^B(\sqrt{\tau}e^{y^*})\cdot q_f^A(\sqrt{\tau}e^{-y^*})]$$

with $\tau = M^2/\sqrt{s}$.

The GRV(LO) parametrization[5] for the structure functions $q_f(x, Q^2)$, taken from PDFLIB package[6], has been adopted since it extends down to quite low values of Q^2 (Q^2_{min}=0.25 GeV/c^2), as needed for NA50 kinematical domain. The isospin composition of the Pb ion is also taken into account.

– p_T: $p_T m_T K_1(m_T/T)$, where K_1 is the second modified Bessel function of order 1, and T=0.236 GeV.

– $cos\theta_{CS}$: 1+cos$^2\theta_{CS}$, since the decaying dimuon has spin 1.

c) $D\overline{D}$

For generation and decay of open charm events the PYTHIA code (version 5.7)[7] has been used in association with JETSET (version 7.4). Since about 80% of open charm comes from gluon-gluon interactions, isospin corrections can be neglected, and only pp collisions have been studied. The dependence of the dimuons' mass distribution on the charm quark mass m_c has been investigated by generating two samples of events, corresponding to the limits of the commonly accepted m_c, namely m_c=1.2 GeV/c^2 and m_c=1.5 GeV/c^2.

Generated events have been followed through the detector simulation program and then their kinematical variables (M, y^*, p_T, $cos\theta$) have been reconstructed using the same procedure applied to experimental data. In order to take into account the smearing effects of the apparatus, the kinematical domain used at generation time ($1.2 \leq M \leq 10$ GeV/c^2, $-0.5 \leq y^* \leq 1.5$, $-0.8 \leq cos\theta \leq 0.8$) is slightly larger than the one used in the analysis.

The reconstructed mass spectra for the four considered processes are presented in fig. 2; the shape of generated DY and $D\overline{D}$ events is also shown, using dashed lines (for J/ψ and ψ' the generated mass is constant and equal to the nominal resonance mass). The reconstructed $D\overline{D}$ spectra corresponding to the two m_c values used at generation time turn out to be quite similar and only the one corresponding to m_c=1.2 GeV/c^2 is shown in fig. 2.

Since the experimental spectrum has to be described as a superposition, with suitable normalizations, of the reconstructed mass spectra shown in fig. 2, 'ad hoc' functions $f_i(M)(i = J/\psi, \psi', DY, D\overline{D})$, which fit the differential spectra, have been introduced.

Finally, the ratio between the number of events accepted by the detector's simulation-reconstruction chain and the number of generated events, in the phase space chosen for the analysis, gives, for each simulated process, the detector's acceptance. The values $A_{DY} = 0.045$ and $A_{D\overline{D}} = 0.015$, which will be used in the following discussion, have been obtained.

3.3. Normalization of the physical processes; DY, J/ψ, ψ'

In the experimental spectrum shown in fig. 1 it is possible to distinguish three different regions, namely:
– a high mass continuum (M≥4 GeV/c^2), which should be mainly due to the Drell-Yan process, since, as shown in fig. 2, this is the only 'continuous' contribution which, due to its slope, extends up to the high mass tail of the spectrum;
– a resonance region (2.7≤M≤4 GeV/c^2), dominated by the decay of $c\overline{c}$ resonances;
– an intermediate mass region (1.5≤M≤2.7 GeV/c^2), where both Drell-Yan and $D\overline{D}$ decay contributions are expected to be important, and also the low mass tail of the J/ψ can play a role.

In this last region it is difficult to disentangle the contributions of the two continuous processes; on the contrary, the remaining part of the spectrum, where the $D\overline{D}$ component (as will be shown later) is negligible, can be fitted in order to obtain the normalization of the other three dimuon sources.

Therefore, for M≥2.9 GeV/c^2, the invariant mass spectrum has been fitted using the function

$$F_{HM}(M) = C_{DY} \cdot f_{DY}(M) + C_{J/\psi} \cdot f_{J/\psi}(M) + C_{\psi'} \cdot f_{\psi'}(M)$$

where the f_is are the functions describing the shapes of the various processes and the C_is are the normalization constants, which are the parameters of the fit. The lower limit of the considered region is chosen as high as necessary to have a negligible $D\overline{D}$ contribution, without loosing accuracy in the determination of the J/ψ normalization. The obtained

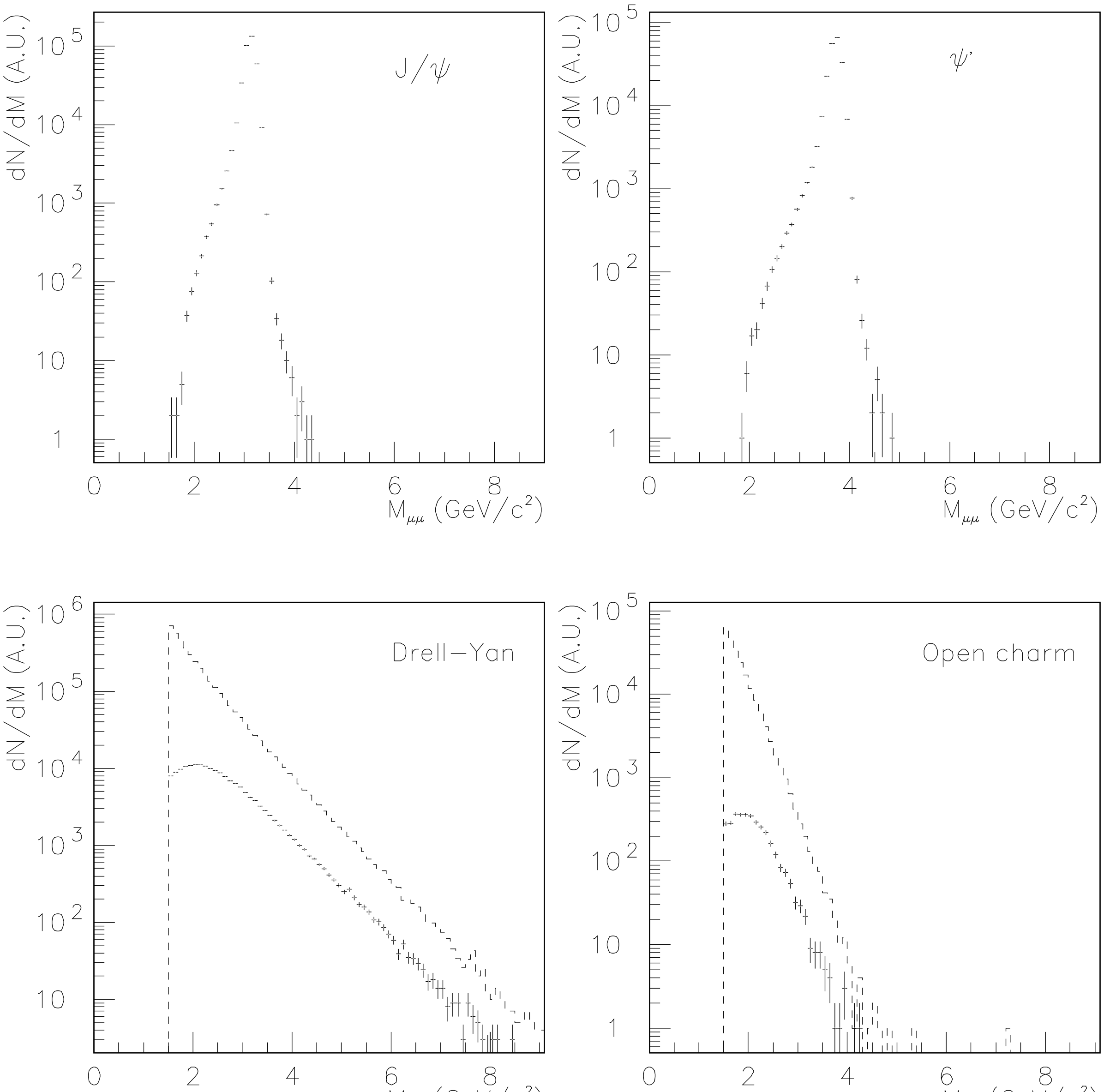

Figure 2. Reconstructed mass spectra from known dimuon sources.

description of the spectrum is satisfactory ($\chi^2/ndf = 1.40$).

Having fixed the normalization constants C_i, the number of events corresponding to DY, J/ψ, ψ' in the experimental mass spectrum can be easily calculated. The Drell-Yan contribution, important for the study of the intermediate mass region, amounts to

$$N_{DY} = \int_{1.5}^{9} C_{DY} f_{DY}(M) dM = (1.62\pm0.05)\cdot 10^4$$

3.4. Normalization of the physical processes; $D\overline{D}$

Although the most direct way to get the open charm normalization would be to start from measured values of $\sigma_{c\bar{c}}$ in nucleon–nucleon collisions at 158 GeV, and then to obtain the expected number of $D\overline{D}$ events in the mass spectrum as:

$$N_{D\overline{D}} = \sigma_{c\bar{c}}^{NN} \cdot \frac{1}{P} \cdot < B.R.(D \rightarrow \mu + X) >^2 \cdot (208)^2 \cdot A_{D\overline{D}} \cdot L$$

(where P is a phase-space factor introduced to take into account the limited kinematical domain where the analysis is performed, $< B.R.(D \rightarrow \mu + X) >$ is the average B.R. for D mesons to decay into a muon plus anything, $A_{D\overline{D}}$ is the acceptance and L is the measured luminosity [1]), here a different approach is followed, which allows to avoid the systematical errors introduced with the use of rather poorly known quantities, as $B.R.(D \rightarrow \mu + X)$ and P.

The normalization of the $D\overline{D}$ component is obtained starting from a preliminary evaluation of the open charm contribution to the dimuon mass spectrum in p–W collisions at 200 GeV (NA38) [8]. In this reference, assuming that known sources accounted for <u>all</u> the dimuon yield, a fit was performed for 1.5≤M≤2.5 GeV/c^2, using the function:

$$F_{1.5\leq M\leq 2.5}(M) = C_{D\overline{D}} \cdot f_{D\overline{D}}^{NA38}(M) + C_{DY} \cdot f_{DY}^{NA38}(M) + C_{J/\psi} \cdot f_{J/\psi}^{NA38}(M) + C_{\psi'} \cdot f_{\psi'}^{NA38}(M)$$

with C_{DY}, $C_{J/\psi}$ and $C_{\psi'}$ fixed from a previous fit to the high mass region, obtaining, both in shape and in absolute normalization, a good description of the spectrum. The value $N_{D\overline{D}}^C/N_{DY}^C = 0.86\pm0.06$ for the acceptance corrected ratio between Drell-Yan and open charm events, in the same kinematical domain now used in this analysis, was obtained[8].

This ratio, for Pb–Pb collisions at 158 GeV per nucleon, can be calculated, starting from NA38 value. The extrapolation from p–W to Pb–Pb is carried out in this way:

$$\left(\frac{N_{D\overline{D}}^C}{N_{DY}^C}\right)_{Pb-Pb}^{200GeV} = \left(\frac{N_{D\overline{D}}^C}{N_{DY}^C}\right)_{p-W}^{200GeV} \cdot \frac{\sigma_{c\bar{c}}^{PbPb200GeV}/\sigma_{c\bar{c}}^{pW200GeV}}{\sigma_{DY}^{PbPb200GeV}/\sigma_{DY}^{pW200GeV}}$$

Since neither Drell-Yan nor open charm production are affected by nuclear absorption effects[9,10] the ratio $\sigma_{c\bar{c}}^{PbPb200GeV}/\sigma_{c\bar{c}}^{pW200GeV}$ is equal to A_{Pb}^2/A_W. However, contrarily to open charm, Drell-Yan process is sensitive to the proportion of protons and neutrons in the nuclei. Taking into account this effect the value $N_{D\overline{D}}^C/N_{DY}^C = 1.01\pm0.07$ is obtained for Pb–Pb collisions at 200 GeV/nucleon.

[1]This method was followed in the oral presentation.

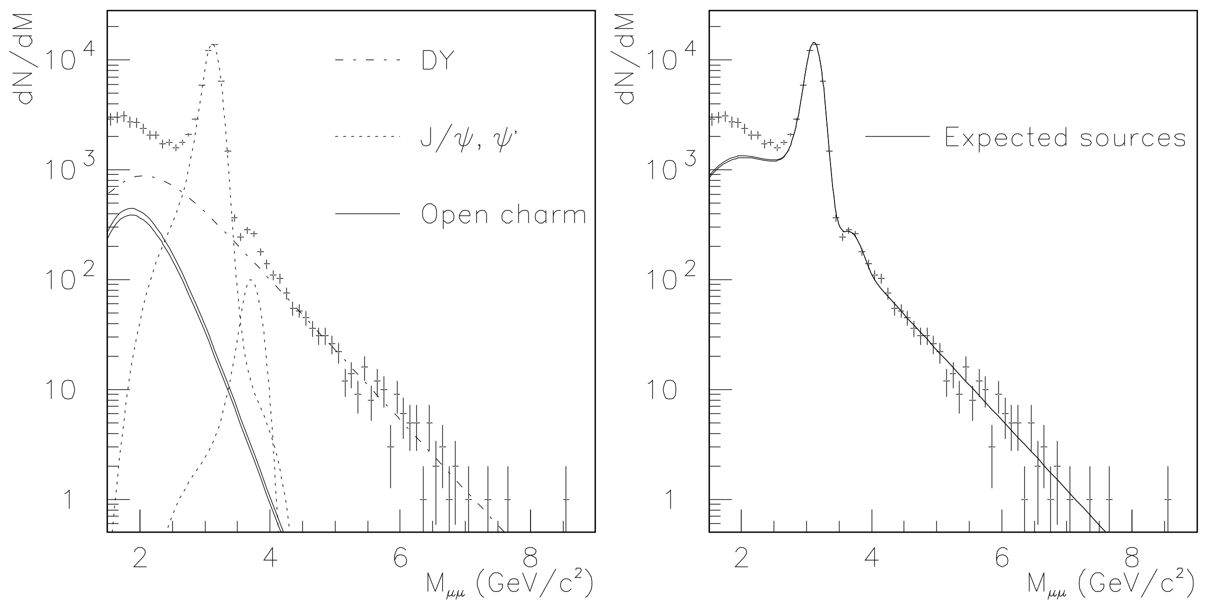

Figure 3. Comparison of measured dimuon yield with expected sources in Pb–Pb collisions.

The energy scaling from 200 GeV to 158 GeV is performed calculating:

$$\left(\frac{N^C_{D\overline{D}}}{N^C_{DY}}\right)^{158GeV}_{Pb-Pb} = \left(\frac{N^C_{D\overline{D}}}{N^C_{DY}}\right)^{200GeV}_{Pb-Pb} \cdot \frac{\sigma^{PbPb158GeV}_{c\overline{c}} / \sigma^{PbPb200GeV}_{c\overline{c}}}{\sigma^{PbPb158GeV}_{DY} / \sigma^{PbPb200GeV}_{DY}}$$

The ratio $\sigma^{PbPb158GeV}_{DY}/\sigma^{PbPb200GeV}_{DY}$ is obtained integrating LO $d^2\sigma/dMdy$ in the region $0 \leq y^* \leq 1$, $M \geq 1.5$ GeV/c^2. For open charm the results of PYTHIA are used. The final value is

$$\left(\frac{N^C_{D\overline{D}}}{N^C_{DY}}\right)^{158GeV}_{Pb-Pb} = 0.82 \pm 0.06$$

Taking now into account the acceptances for the two processes and the N_{DY} value obtained in the previous section, it turns out that in the 'signal' spectrum $N_{D\overline{D}} = (4.5 \pm 0.3) \cdot 10^3$ events, with the mass shape showed in fig. 2, originate from open charm decays.

3.5. Results

In fig. 3 the calculated contribution of each of the four processes to the dimuon mass spectrum is shown, as well as their sum. For open charm decays, the two solid lines correspond to the expected production $\pm 1\sigma$. It is evident that known sources in the intermediate mass region underestimate the experimentally measured yield. The size of the excess can be quantified using the ratio *Data / Expected sources*. For Pb–Pb collisions at 158 GeV/nucleon, in the mass region $1.5 \leq M \leq 2.5$ GeV/c^2, the value *(Data / Expected*

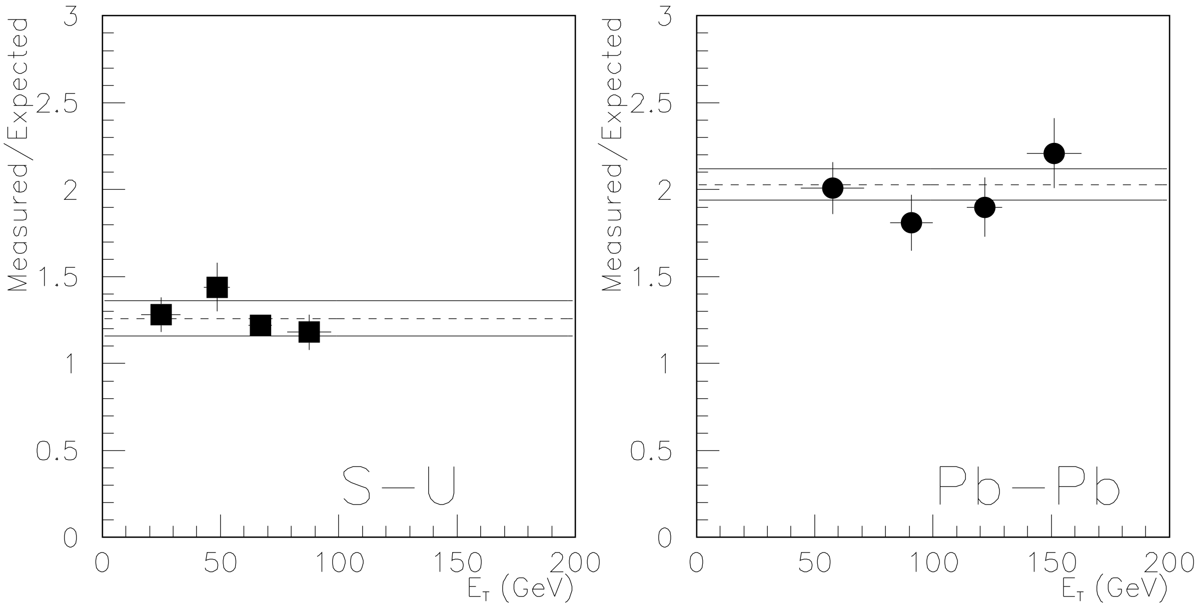

Figure 4. Centrality dependence of the excess in S–U (NA38) and Pb–Pb (NA50)

sources)^{PbPb} = 2.03±0.09 is obtained. A similar analysis, carried out on NA38 S–U interactions at 200 GeV/nucleon, gave *(Data / Expected sources)*^{SU} = 1.26±0.10 [8].

4. CENTRALITY DEPENDENCE OF THE EXCESS

In NA50 the centrality of the collision can be estimated in three different ways, namely by the measurement of neutral transverse energy E_T in the EMC, of forward energy (ZDC) and of charged hadron multiplicity (MD). For this analysis the 'signal' E_T spectrum corresponding to the intermediate mass region has been subdivided in four equipopulated bins, corresponding to the E_T intervals $E_T \leq 77$ GeV, $77 < E_T \leq 108$ GeV, $108 < E_T \leq 135$ GeV, $E_T > 135$ GeV, the last bin corresponding to the most central events.

A check of the performance of the EMC detector has been obtained verifying that spectra for the three NA50 centrality detectors were mutually correlated.

The invariant mass spectrum corresponding to each E_T bin has then been analyzed following the procedure described in section 3, and assuming that the quantity $N^C_{D\overline{D}}/N^C_{DY}$ does not depend on centrality.

The result, expressed again as *(Data / Expected sources)* for the mass interval $1.5 \leq M \leq 2.5$ GeV/c^2, is shown in fig. 4, where also the centrality dependence of the excess measured by NA38 in S–U collisions, is plotted[8]. It has to be noted that NA38 EMC measured neutral transverse energy in a different pseudorapidity domain, namely $1.7 < \eta < 4.1$. The lines in the plots show the E_T integrated results described in section 3.5.

5. CONCLUSIONS

The intermediate mass muon pair continuum measured by NA50 experiment in Pb–Pb collisions at 158 GeV/c cannot be described in terms of known dimuon sources, which underestimate the total yield by a factor of about 2. Such an effect was already seen in S–U collisions by NA38[8] and HELIOS/3[11] experiments.

The observed excess does not exhibit a clear trend as a function of the centrality of the collision.

REFERENCES

1. L. Anderson et al., Nucl. Inst. Meth. 223(1984) 26.
2. E. Chiavassa et al., Nucl. Inst. Meth. A367(1995) 267.
3. B. Alessandro et al., Nucl. Inst. Meth. A360(1995) 189.
4. A. Borhani, PHD thesis, Universite Paris VI, 1996.
5. M. Gluck, E. Reya, A. Vogt, Z. Phys. C53(1992) 127.
6. H. Plothow-Besch, Comp. Phys. Comm. 75(1993) 396.
7. T. Sjostrand, Comp. Phys. Comm. 82(1994) 74.
8. C. Lourenço, PHD thesis, Universidade Tecnica de Lisboa, 1995.
9. A.S. Ito et al., Phys. Rev. D23(1981) 604.
10. G.A. Alves et al., Phys. Rev. Lett. 70(1993) 722.
11. M. Masera for the HELIOS/3 collaboration, Nucl. Phys. A590(1995) 93c.